2-1983

Bathymetric Prediction from SEASAT Altimeter Data

Timothy H. Dixon
thd@usf.edu

M. Naraghi

M. K. McNutt

S. M. Smith

JOURNAL OF GEOPHYSICAL RESEARCH, VOL. 88, NO. C3, PAGES 1563–1571, FEBRUARY 28, 1983

Bathymetric Prediction From SEASAT Altimeter Data

T. H. DIXON AND M. NARAGHI

Jet Propulsion Laboratory, Pasadena, California 91109

M. K. MCNUTT[1]

U.S. Geological Survey, Menlo Park, California 94025

S. M. SMITH

Geological Research Division, Scripps Institution of Oceanography, La Jolla, California 92093

The linear response function technique is used to analyze two 1300-km tracks of SEASAT altimeter data and corresponding bathymetry in the Musician Seamounts region north of Hawaii. Bathymetry and geoid height are highly correlated in the 50- to 300-km wavelength range. A predictive filter is developed which can operate on SEASAT altimetry in poorly surveyed oceanic regions to indicate the presence of major bathymetric anomalies. Modeling of the bathymetry-geoid correlation in the Musician region is attempted using the elastic plate model. The flexural rigidity D of the plate is not well constrained by our data but appears to lie in the range 5×10^{21} N m – 5×10^{22} N m at the time of loading. Since the Musician Seamounts and the crust on which they lie are both Late Cretaceous in age, this value represents the effective flexural rigidity of very young lithosphere that was 'frozen in' at the time of volcanism. The modeling indicates that the general form of a predictive filter will strongly depend on various geologic parameters, especially the effective flexural rigidity. Hence, some a priori geologic constraints are necessary to estimate successfully the bathymetry from the altimeter data. Alternately, if high-quality bathymetry is available, a crude estimate of the age of loading (i.e., volcanism) can be made from the altimeter data.

INTRODUCTION

The surface of the ocean is a good approximation to the marine geoid, a gravitational equipotential surface defined by mean sea level. If the western boundary currents and near-shore areas are ignored, time-varying deviations of sea surface height from the geoid, caused by currents, storms, or mesoscale eddies, are typically less than 50 cm [e.g., *Wunsch and Gaposchkin*, 1980].

Since geoid anomalies decrease slowly with distance r from a mass anomaly (proportional to r^{-1}), the shape of the geoid reflects the distribution of a relatively deep-seated mass within the earth. The vertical gradient of the potential, the gravitational field, decreases more rapidly (proportional to r^{-2}) and hence is more sensitive to shallow mass anomalies. Nevertheless, a major contribution to the marine geoid is made by topographic anomalies in the very shallow rock-water interface at the base of the ocean, since this surface represents a large density contrast. Consequently, there is a strong correlation between the shape of the geoid and ocean bottom topography (bathymetry).

NASA's SEASAT satellite acquired high-precision altimeter data with near-global coverage, providing new, detailed geoid information. A mission overview is given by *Born et al.* [1979]. The SEASAT orbit is known to a good approximation; in any case, orbital tracks respond only to wavelength components of the gravitational field longer than many features of geologic interest. Other radial orbit uncertainties, cause by poorly modeled atmospheric drag and radiation pressure, are also long-wavelength effects. Thus variations in satellite height above the ocean surface are a good measure of short- and medium-wavelength geoid variation.

In principle, it is possible to use the bathymetry-geoid correlation to predict bathymetry from satellite altimeter data. That such a predictive tool might be useful is apparent by inspection of existing bathymetric charts, especially in the South Pacific where ship crossings are rare. Large areas are known to no better than 100-km resolution; hence many first-order features such as seamount chains, fracture zones, plateaus, and basins may be undetected at present.

In addition to predicting bathymetry in unsurveyed areas, the altimeter data allow geophysical modeling in areas where bathymetry is well known. The observed geoid response to topography contains information about the compensation mechanism as well as the relative densities of the loads (e.g., seamounts) and underlying mantle. Since the latter two parameters are reasonably well known, details of the compensation mechanism can be investigated.

This paper describes a feasibility study of a predictive bathymetry technique using SEASAT altimeter data. A test area in the Musician Seamounts province north of Hawaii was used (Figure 1). Since this region occurs near the central part of the mid-latitude anticyclonic gyre, surface currents are not strong. In addition, high-quality bathymetric data are available. As we shall show, the observed geoid response for a given bathymetric anomaly in this region is probably near a minimum for oceanic crust. Consequently, the area represents a severe test for bathymetric prediction.

PREVIOUS WORK

A number of studies in the ocean basins have indicated that the gravitational field or geoid are correlated with

[1] Now at Department of Earth Science, Massachusetts Institute of Technology, Cambridge, Massachusetts 02139.

Paper number 2B1446.
0148-0227/83/002B-1446$05.00

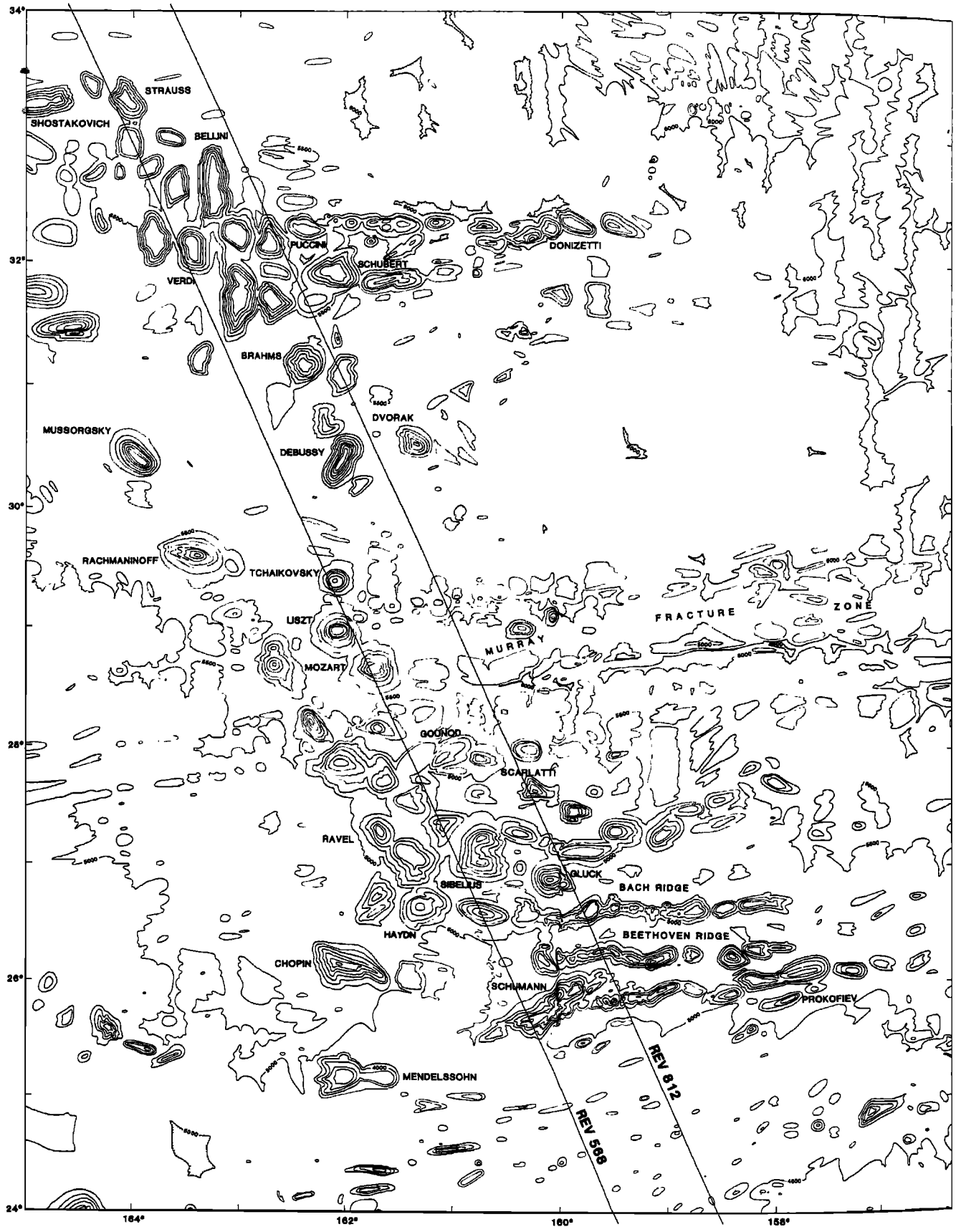

Fig. 1. Generalized bathymetry of the Musician Seamounts area north of Hawaii. Contour interval is 500 m. Portions of the two SEASAT data tracks used in this study are indicated with solid lines.

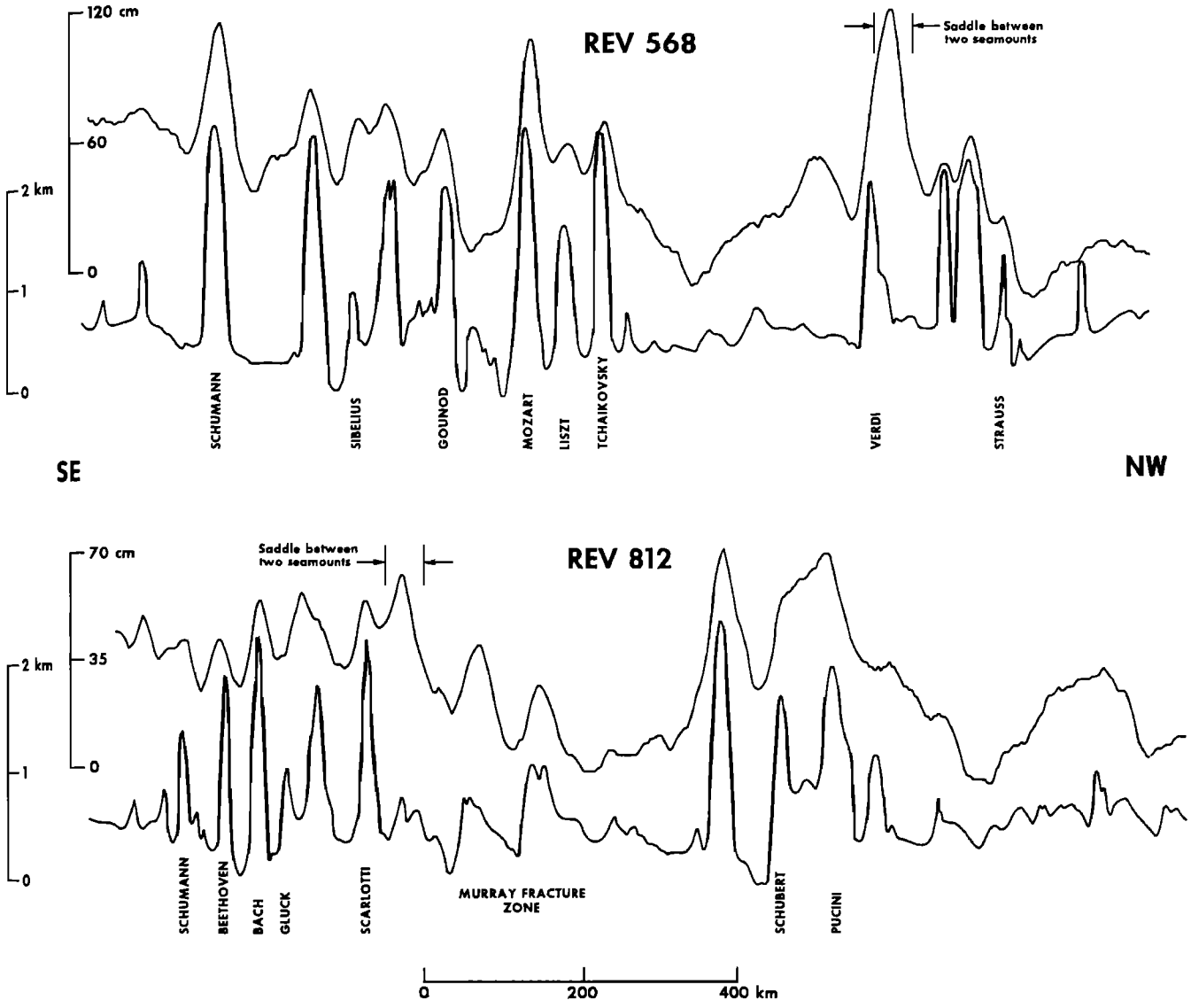

Fig. 2. Altimeter data and bathymetry corresponding to the two data tracks in Figure 1. Altimetry has been high-pass filtered and smoothed, while bathymetry has only been high-pass filtered.

bathymetry at short to medium wavelengths (30–300 km [*Talwani et al.*, 1972; *McKenzie and Bowin*, 1976; *Watts*, 1978, 1979; *McNutt*, 1979]). Time series analysis on the two correlated data sets, involving computation of a linear response function, allows a quantitative description of this relation [*Dorman and Lewis*, 1970]. A filter f is constructed which, when convolved with bathymetry b, produces a series resembling gravity or geoid data g. In the wave number domain this is described by

$$G(k) = Q(k) \cdot B(k) + n \tag{1}$$

where G, Q, and B are the discrete Fourier transforms of g, f, and b; n represents noise; and k is the absolute value of the wave number. Q is the response function, and the required predictive filter is the inverse Fourier transform of the reciprocal of Q. This concept is used here to derive a predictive filter for bathymetry with SEASAT altimeter data as an input. This approach assumes that the response function is linear, stationary, and isotropic (see *McNutt* [1979] for a more detailed discussion). Although, in general, this may not be true, we will show that it is justified within the boundaries of a single geologic province such as the Musician Seamounts.

McKenzie and Bowin [1976] first applied this type of analysis to oceanic data. To minimize problems associated with noise and resulting filter instability, these authors split a long, one-dimensional data track into a series of equal-length smaller tracks and computed a new response function (termed the admittance, Z) from the cross spectra of the gravity and topography data and the power spectra of bathymetry:

$$Z(k) = |\Sigma(G_i B_i^*)|/\Sigma B_i B_i^* \tag{2}$$

B^* is the complex conjugate of B, and the summations are taken from $i = 1$ to M, the number of data sets.

Comparison of admittance functions to theoretical response functions has shown that the compensation of ocean bottom topography is best explained by a regional mechanism. Such compensation can be modeled with thin elastic plate theory in which loads are supported by a rigid plate overlying a weaker asthenosphere [e.g., *Walcott*, 1970; *McNutt and Menard*, 1978]. An important parameter is the

strength of the plate or flexural rigidity D. *Watts et al.* [1980] have shown that D increases as the lithosphere ages and cools.

Clague and Dalrymple [1975] dated two seamounts in the Musician province. They report ages of 65 and 87 m.y., respectively, or somewhat younger than the age of the surrounding seafloor (~85–95 m.y. [e.g., *Heezen and Fornari*, 1975]). The boundaries of this seamount province show no displacement across the Murray Fracture Zone (Figure 1). Since this fracture zone represents a very large offset (~10 m.y. or 1000 km at a 10 cm/yr spreading rate) this suggests that the Musician Seamounts were formed in an intraplate setting, albeit near a ridge crest [*Menard and McNutt*, 1982].

Data Analysis

Two tracks of SEASAT altimeter data over the Musician Seamounts were used, each track approximately 1300 km long (Figure 1). Both data sets were from ascending passes, i.e., satellite track southeast to northwest. They were acquired August 5 and August 22, 1978, (day 217 and 234 of the SEASAT mission), on orbital revolutions 568 and 812.

High-resolution bathymetry of the region is available, based on the U.S. Navy Seamap Project, 1961–1970 [NOAA, 1973]. North-south ship tracks have an average spacing of 15 km, with east-west tie lines spaced at approximately 100 km. The data have been contoured at a 100-m contour interval. Bathymetry corresponding to the satellite track were digitized from the published charts at 3.5-km spacing. The original altimeter data represented one per second averages (7-km spacing) of 10-Hz data, which were then interpolated back to 3.5-km spacing to match the bathymetry sample interval.

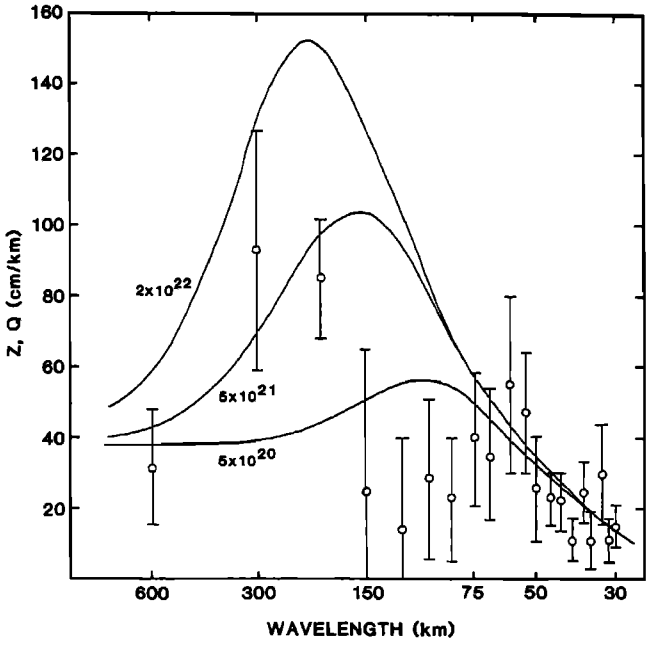

Fig. 3. Computed response estimates (Z) generated from the altimetry and bathymetry in Figure 2. The length of an individual error bar (plus or minus) represents the quantity σ_Q, where $(\sigma_Q)^2 = (1/M)\,[(\Sigma G_i^2/\Sigma B_i^2) - Q^2]$, using the symbols defined for equation (1) and (2) in text. Solid lines represent theoretical response functions (Q) for the elastic plate model (equation (3) in the text) with variable flexural rigidity D. The following parameter values were used: Z_1 = 4 km; Z_2 = 10 km; ρ_1 = 2600 kg/m^3, ρ_2 = 3300 kg/m^3.

The altimeter values used were obtained from the standard SEASAT geophysical data record [*Brown et al.*, 1979]. They represent sea height with respect to the reference ellipsoid [*Moritz*, 1979] corrected for instrument effects and containing three corrections for variable index of refraction in the atmosphere: ionospheric correction [*Wu*, 1977; *Lorrell et al.*, 1982] and wet and dry tropospheric correction [*Saastamoinen*, 1972; *Tapley et al.*, 1982*a*] based on Fleet Numerical Oceanographic Center (FNOC) meteorological data. No tidal or other corrections were employed. The altimeter precision is approximately 10 cm [*Tapley et al.*, 1982*b*].

The altimeter data contain long-wavelength (>300 km) trends, which probably represent deep-seated mass anomalies. Since these wavelengths are longer than the range where bathymetry and the geoid are correlated, both the altimeter and bathymetric data were detrended. Figure 2 shows both data sets after trend removal and smoothing. Trend removal was accomplished by subtracting a 100-sample (350 km) moving average from each data point. The detrended altimeter data were then smoothed with a five-sample (18 km) moving average to reduce noise. The wavelength components of critical interest (30–300 km) are unaffected by this combination of high- and low-pass filters.

In order to calculate the admittance Z according to equation (2), each of the two 1300-km data tracks was split into two equal-length subtracks. The function Z, in centimeters of sea height per kilometer of seafloor topography, is shown in Figure 3.

Figure 3 also shows theoretical response functions, calculated for a simple one-layer elastic plate model with variable D. The geoid response for such a model is given by

$$Q(k) = \frac{G\rho_1}{gk}\left\{\exp(-2\pi k Z_1) - \cdot\left[1 + \frac{16\pi^4 k^4 D}{g(\rho_1 - \rho_2)}\right]^{-1}\exp(-2\pi k Z_2)\right\} \quad (3)$$

Banks et al. [1977] and *McNutt* [1979] give the gravity-equivalent form of this equation. Z_1 and Z_2 represent the respective distances from the observation plane (ocean surface) to the mean ocean bottom and plane of major density contrast in the plate (Mohorovicic discontinuity). The ρ_1 and ρ_2 represent the density of topography and underlying mantle, and G and g are the gravitational constant and acceleration, respectively.

Although the one-dimensional data used here are not sufficient to constrain D tightly, comparison of the theoretical response $Q(k)$ to the observed response $Z(k)$ does place upper and lower bounds on its value (Figure 3). On this basis, flexural rigidity in the Musician Seamounts region must be less than 3×10^{22} N m. This upper limit is an order of magnitude lower than values calculated for oceanic crust of similar age and, in fact, represents flexural rigidity at the time of loading. *Watts* [1979] used GEOS 3 altimeter data to compute elastic plate thickness T_e for the Hawaiian Ridge (a recent load on old crust) equal to 28 to 37 km. Since

$$D = \frac{ET_e^3}{12(1 - \sigma^2)} \quad (4)$$

where E is Young's modulus $\simeq 8 \times 10^{10}$ N/m^2 and σ is Poisson's ratio $\simeq 0.27$, this range of plate thickness corresponds to $D \simeq 2$–3×10^{23} N m. Estimates of D for young Pacific lithosphere range from 5×10^{20} N m [*McNutt*, 1979] to 1×10^{21} N m [*Cochran*, 1979]. Available data indicate that the Musician Seamounts probably formed between 5 and 30 m.y. after crustal formation at a ridge crest. The variation of D with crustal age at the time of loading is known approximately [*Watts et al.*, 1980]. D should be in the range of 5×10^{21} to 5×10^{22} for the Musician Seamounts, which agrees with the admittance values calculated here (Figure 3).

The admittance values for longer wavelengths (200–300 km) suggest higher values of flexural rigidity than do the shorter wavelength terms. Although our results are not conclusive, one possible explanation is that longer-wavelength features are not well described solely by a static compensation model. Longer-wavelength topography may result from elastic response to loads at the base of the plate [*McNutt*, 1982]. It is possible that the anomalous response in the spectral region between 200 and 300 km represents dynamically maintained topography due to convective processes in the mantle.

Bathymetric Prediction

The admittance function calculated from the Musician Seamounts data could be inverted to yield a predictive filter for bathymetry. However, such a filter would not have general application except in areas with similar geologic characteristics. A better approach is to invert a theoretical response function. These can be constructed for any oceanic region, assuming that some a priori geologic knowledge is available to constrain the parameters in equation (3). The sensitivity of the bathymetric prediction to various parameter choices can also be tested.

Figure 4 represents the detrended and smoothed altimeter data passed through a filter, derived by inversion of a theoretical response function (equation (3)) similar to those in Figure 3. Thus bathymetry is treated as an unknown and predicted, assuming an effective flexural rigidity of 10^{22} N m. For comparison, the original (but detrended) bathymetry is also shown, along with the residuals (observed minus predicted). Figure 5 shows the dependance of the response function on density of topography (ρ_1) and depth to the Mohorovicic discontinuity (Z_2). Figure 6 shows the sensitivity of the bathymetric prediction to variation in three critical parameters in equation (3), namely D, ρ_1, and Z_2.

By inspection of Figures 5 and 6, it is apparent that the bathymetry prediction is sensitive to the choice of Z_2 only at long wavelengths. This type of spectral dependence is expected for regional compensation. The compensating mass will have larger lateral dimensions than the topographic load and so will only influence the response function and the bathymetric prediction at long wavelengths.

The prediction exhibits moderate sensitivity to ρ_1. While Z_2 is a long-wavelength effect, the spectral influence of ρ_1 persists at short wavelengths, i.e., seamount dimensions. The predicted height of seamounts varies by approximately ± 500 m for a geologically reasonable range of densities.

The prediction is strongly influenced by the choice of D, the effective flexural rigidity, i.e., D at the time of loading. This is due to the high sensitivity of the response function at medium wavelengths to the value of D (Figure 3). In the absence of age information on the Musician Seamounts, this parameter could only be constrained between 5×10^{20} N m (D for new lithosphere) and 2×10^{23} N m (D for mid-Cretaceous seafloor). Figure 6 indicates that variation of D between 10^{21} N m and 10^{23} N m results in the bathymetric prediction varying as much as 1.0 km.

The predictive filter is obtained with an inverse Fourier transform (F^{-1}) of Q. To compensate for a low signal-to-noise ratio at higher frequency and consequent filter instability, terms corresponding to wavelengths shorter than 20 km (k_c) in the inverted filter were set to zero. This is equivalent to generating a new response function $\hat{Q}(k)$ by multiplying the original function $Q(k)$ by a box function Π, where

$$\Pi(k) = 1 \qquad |k| \leq k_c$$

$$\Pi(k) = 0 \qquad |k| > k_c$$

Thus

$$\begin{aligned} \hat{f}(x) &= F^{-1}\, \hat{Q}(k) \\ &= F^{-1}\, Q(k)\Pi(k) \\ &= f(x) * \frac{\sin(2\pi k_c x)}{2\pi k_c x} \end{aligned} \tag{5}$$

We can therefore expect to see some artifacts in the predicted bathymetry with variation proportional to $[\sin(x)]/x$. This is especially apparent adjacent to high-amplitude, short-wavelength features such as seamounts and would vary with the exact cutoff frequency used (e.g., adjacent to Verdi Seamount, Figure 4*a*).

Discussion

The data sets in Figure 2 show obvious high correlation. The major exceptions occur as a result of the one-dimensional nature of the data. Where the satellite track passes adjacent to a seamount, or in a saddle between two seamounts, a positive geoid anomaly is recorded, while the corresponding bathymetric anomaly, displaced off track, is not. Two examples of this effect are labeled in Figure 2 (compare to Figure 1) on rev 568 (near Verdi Seamount) and rev 812 (northwest of Scarlotti Seamount). In general, this is not a severe problem in the data sets shown because the topography is somewhat lineated, at least at longer wavelengths, and the chosen satellite tracks are approximately perpendicular to this trend. It, nevertheless, causes the major uncertainty in the predictive filter for bathymetry.

By inspection of Figures 1 and 4, it is apparent that the largest residuals in the bathymetric prediction are also due solely to off-track feature location. Since a positive geoid anomaly is recorded in the altimeter data with little or no corresponding bathymetric anomaly for satellite passes adjacent to a seamount, the predicted bathymetry will be positive, causing a large positive residual. In rev 812 (Figures 1 and 4*b*), this effect is observed for an unnamed seamount immediately northwest of Scarlotti. Three examples occur in the rev 568 data at Sibelius, Liszt, and Verdi seamounts.

The residual associated with the Verdi prediction is the largest observed due to an additional effect. Here, the satellite track actually passes in the saddle between two seamounts. Moreover, these seamounts are not symmetric in their cross-track location. Verdi is located to the south-

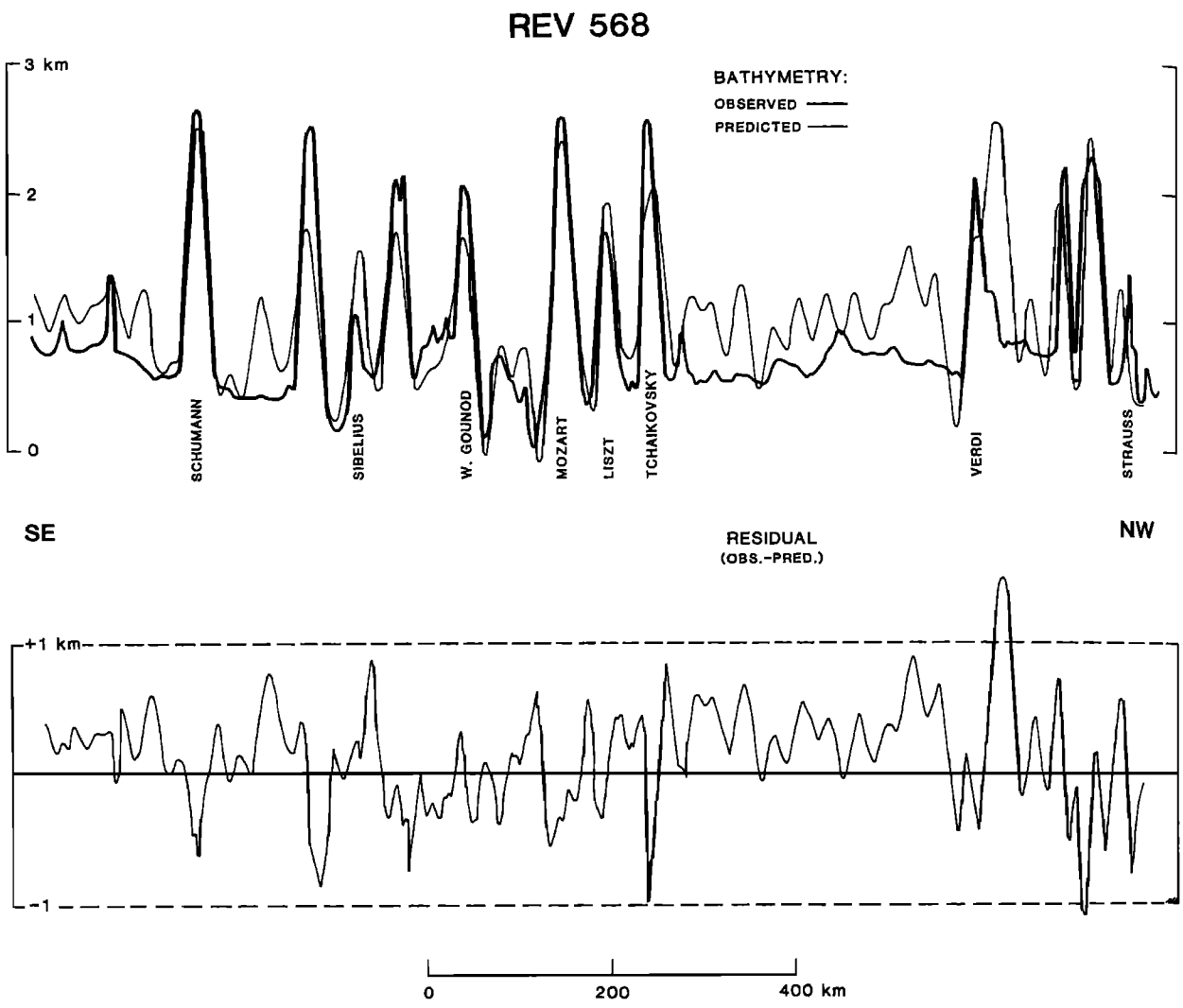

Fig. 4*a*

Fig. 4. Predicted bathymetry, using detrended and smoothed altimeter data (Figure 2) as an input to a filter derived from an inverted theoretical response function (equation (3)) similar to those in Figure 3. $D = 1 \times 10^{22}$ N m, and the remaining parameter values are those of Figure 3. The actual and the residual (observed-predicted) bathymetry are also shown. Double vertical lines in Figure 4*b* at Beethoven and Bach Ridge bracket high-amplitude, short-wavelength residuals (both positive and negative) and are located at positions of zero residual. These large residuals are due to significant bathymetric anomalies immediately adjacent to the satellite track, which cause the predicted peak to be out of phase with the observed peak. The vertical lines marking the seamount immediately NW of Scarlotti only bracket a positive residual, since adjacent bathymetry is perpendicular to track and the prediction is in phase.

east, while a large unnamed seamount is located northwest (Figure 1). Consequently, the local peaks in the geoid and bathymetry do not coincide, and a large positive bathymetric feature is predicted northwest of the recorded one-dimensional bathymetric high associated with the west flank of Verdi. The rev. 812 prediction (Figure 4*b*) also has large residuals (both positive and negative) due to off-track mass anomalies that are not perpendicular to the local bathymetric anomaly. The satellite track crosses Bach and Beethoven ridges nearly perpendicular to their regional trend, but at a location where major bends in these ridges occur (Figure 1). In the case of Beethoven Ridge, the topographic high is displaced southward in that portion of the local ridge, which is east of the satellite track. The positive geoid anomaly associated with this feature is therefore located southeast of the recorded subsatellite bathymetric peak. Consequently, the predicted bathymetric peak is southeast of the actual subsatellite peak, and the corresponding residual is first positive, then negative (Figure 4*b*). The reverse situation occurs over Bach Ridge, where the local geoid high is displaced several kilometers northwest of the recorded bathymetric high.

When the satellite track passes near the center of a seamount, the predicted bathymetric height will be less than the actual height, causing a negative residual. This is also a consequence of the one-dimensional approximation, since the actual conical seamount has mass deficiencies to both right and left of the satellite track relative to the assumed infinite two-dimensional ridge. Thus the observed positive geoid anomaly is less than expected, and the corresponding

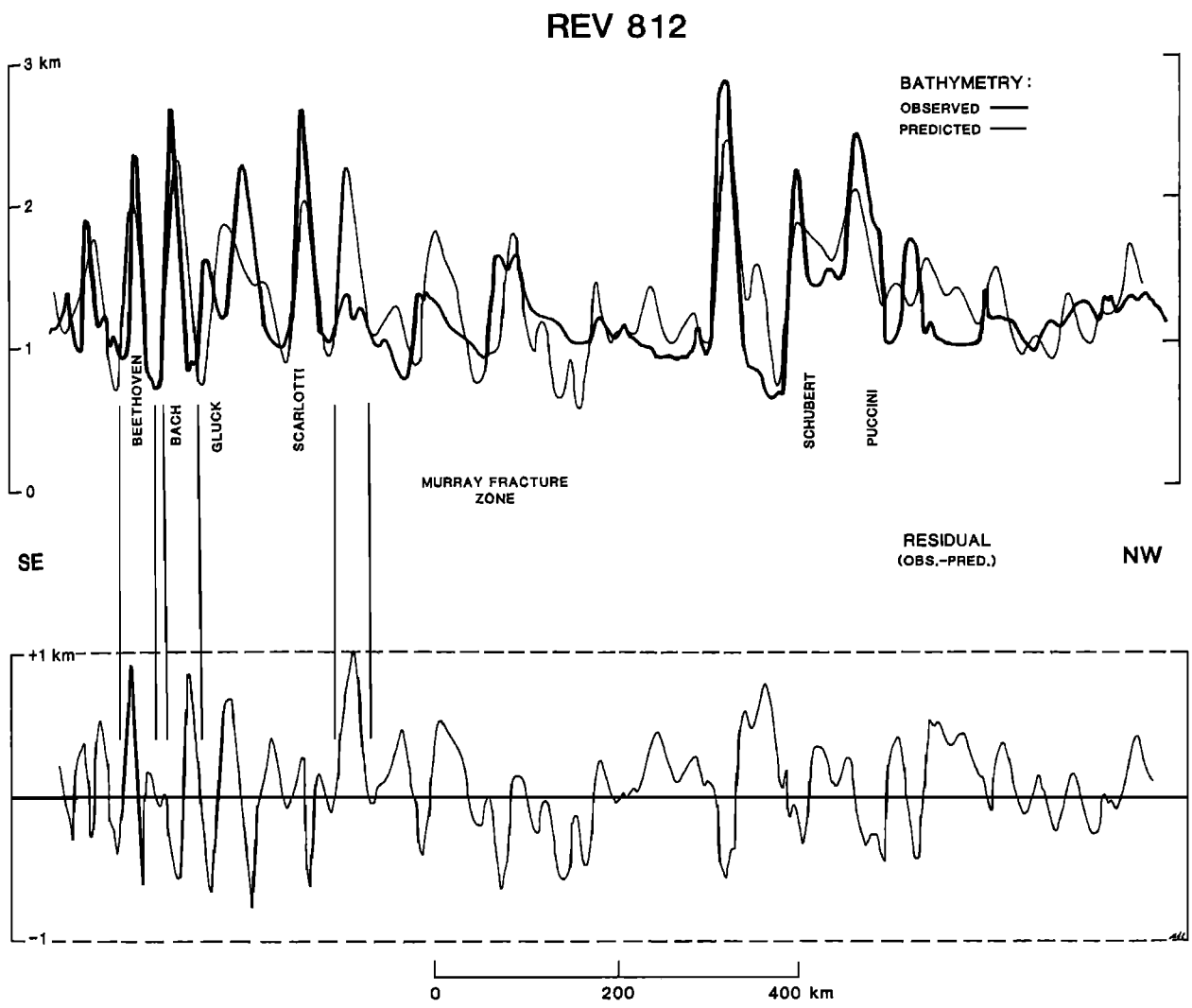

Fig. 4*b*

height prediction is low. Examples in rev 568 are the seamounts immediately north and south of Sibelius and Tchaikovsky Seamount. In rev 812, Scarlotti and the unnamed seamount southeast of Brahms (Figure 1) and south of Schubert have significant negative residuals due to this effect.

Residuals in the predicted bathymetry which are not due to off-track feature location are almost invariably less than 500 m. The magnitude of such residuals indicates the degree of nonstationarity of the response function, while the sign of the residual suggests the origin of the nonstationary process. For example, if a particular seamount was characterized by local compensation, or regional compensation with low effective D, it would cause a smaller positive geoid anomaly relative to a regionally compensated seamount with high effective D. If the predictive filter for bathymetry assumes regional compensation with high effective D, then the predicted bathymetry over the feature will be too low, and the residual (observed-predicted) will be negative. Conversely, if local compensation is assumed for the filter and, in fact, a particular feature is regionally compensated (e.g., a young seamount on old crust), then the prediction will be too high and the residual positive. Since residuals not due to obvious off-track feature location are low, the assumption of a linear, stationary, and isotropic response function seems justified for the region covered by this study [cf. *Schwank and Lazarewicz*, 1982].

In general, the relatively sparse SEASAT data set does not allow two-dimensional analysis. A possible exception occurs near the northern and southern limits of the SEASAT orbital track (~65°–70° latitude) where converging orbits generated a dense network of crossing arcs. Although wave heights tend to be higher here, introducing some uncertainty into the altimeter measurement, the bias can be adequately corrected [*Born et al.*, 1982; *Douglas and Agreen*, 1981; *Hayne and Hancock*, 1982]. For altimeter applications involving seamount location in poorly surveyed areas, the large residuals associated with the one-dimensional aspect of the SEASAT data are not necessarily a major problem. The predicted features actually exist in close proximity (±20 km) to the subsatellite track location.

At least two large positive residuals in Figure 4 could be due to the presence of hitherto undetected topographic features. In rev 568 data, positive sea height anomalies

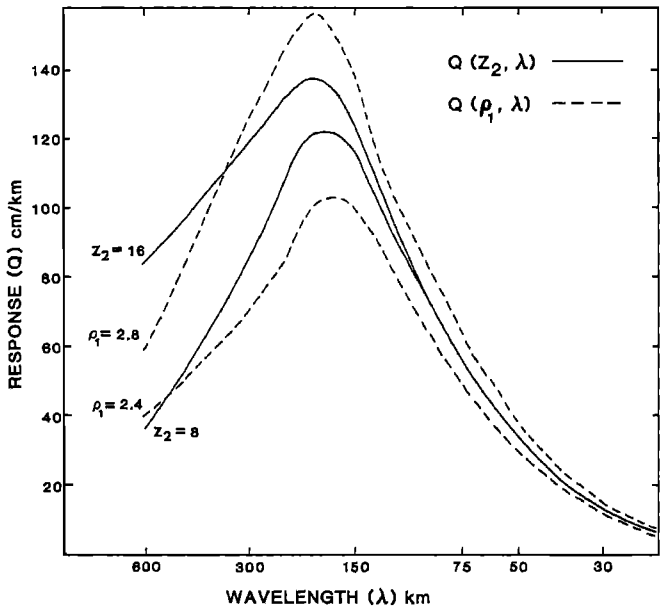

Fig. 5. Variation in the response function Q (equation (3) in the text) as a function of topographic density ρ_1 and depth of compensation Z_2. Note that ρ_1 affects the response at short wavelength, while Z_2 only affects long-wavelength response. For $Q(Z_2, \lambda)$, $\rho_1 = 2600$ kg/m^3. For $Q(\rho_1, \lambda)$, $Z_2 = 10$ km. For both functions, $D = 10^{22}$ N m, and the remaining parameters are the same as for Figure 3.

(Figure 2) and corresponding positive bathymetric predictions (Figure 4*a*) occur immediately northwest of Schumann Seamount and southeast of Verdi Seamount. Inspection of the original bathymetric data indicates that ship track spacing would not be adequate to resolve the presence of these postulated features.

Available age data indicate that both the Musician Seamounts and the crust on which they lie are Late Cretaceous in age. Thus the Musician Seamounts formed near a ridge crest, when the effective flexural rigidity was presumably near a minimum. Without knowing the age of loading, the observed (i.e., relatively low) geoid response above the Musician Seamounts could be used to infer a formation time close to the formation of underlying seafloor. *Watts et al.* [1980] used surface gravity data in much the same way to infer formation ages for a variety of seamount provinces in the Pacific.

The corollary to this is that some a priori geologic constraints are necessary to predict bathymetry successfully. The relatively low geoid response in the Musician region, typically less than 1 m over the larger seamounts (Figure 2), is near the minimum for the ocean basins and represents the least favorable condition for bathymetric prediction. A very different case would exist for young intraplate volcanoes, which represent recent loads on older rigid oceanic crust. By inspection of the models in Figure 3 and the predictions in Figure 6 it is apparent that the amplitude of the ocean surface response to a seamount load varies greatly with the effective flexural rigidity, which, in turn, varies with crustal age. Geoid height anomalies for the case of recent loading on old crust can be 2 to 3 times higher for a given bathymetric anomaly of seamount dimension, relative to the Musician case. Clearly, geologic constraints or assumptions in a given area are necessary before reasonable bathymetric predictions can be made from the altimeter data.

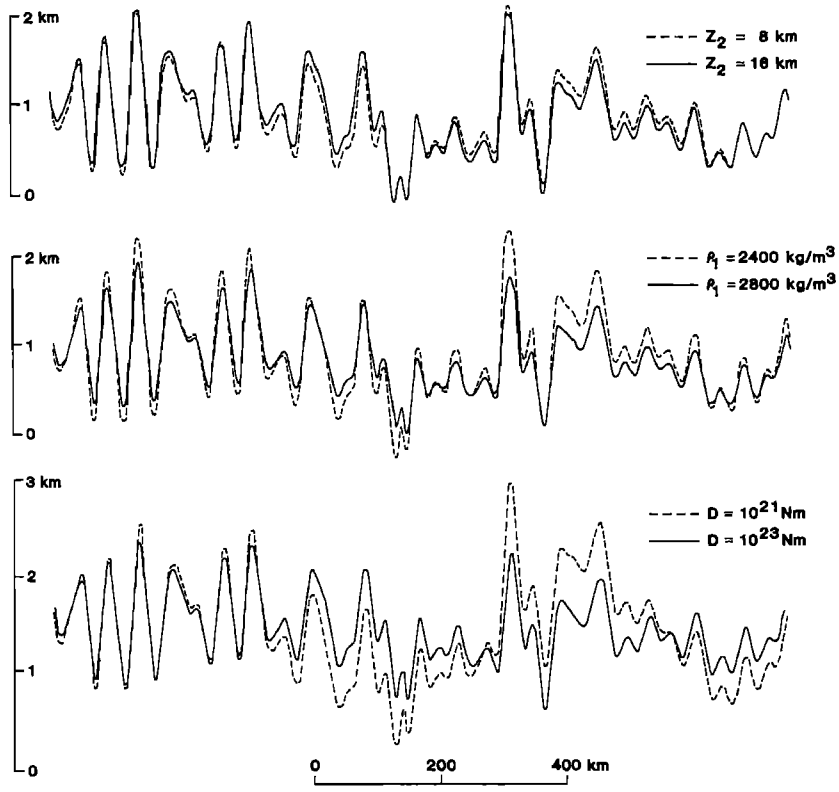

Fig. 6. Variation in the bathymetric prediction as a function of the topographic density ρ_1, flexural rigidity D, and depth of compensation Z_2 in equation (3). See Figures 3 and 5 for the resulting response functions. Predictions have been plotted at the same mean depth. Note that the prediction is particularly sensitive to the effective flexural rigidity, which, in turn, depends on the relative ages of the crust and topographic load.

Acknowledgments. This research was carried out at the Jet Propulsion Laboratory, California Institute of Technology, under contract with the National Aeronautics and Space Administration. We thank M. Richards, R. Stewart, A. Loomis, M. Parke, and J. Solomon for help and advice during various phases of the work. Comments by two anonymous reviewers greatly improved the manuscript.

REFERENCES

Banks, R. J., R. L. Parker, and S. P. Huestis, Isostatic compensation on a continental scale: Local versus regional mechanisms, *Geophys. J. R. Astron. Soc., 51,* 431–452, 1977.

Born, G. H., J. A. Dunne, and D. B. Lame, Seasat mission overview, *Science 204,* 1405–1406, 1979.

Born, G. H., M. A. Richards, and G. Rosborough, An empirical determination of the effects of sea state bias on SEASAT altimetery data, *J. Geophys. Res., 87,* 3221–3226, 1982.

Brown, J. W., G. C. Cleven, J. C. Klose, D. B. Lame, and C. A. Yamarone, Seasat low-rate data system, *Science, 204,* 1407–1408, 1979.

Clague, D. A., and G. B. Dalrymple, Cretaceous K-Ar ages of volcanic rocks from the Musicians Seamounts and the Hawaiian Ridge, *Geophys. Res. Lett., 2,* 305–308, 1975.

Cochran, J. R., An analysis of isostasy in the world's oceans, 2, Midocean ridge crests, *J. Geophys. Res., 84,* 4713–4729, 1979.

Dorman, L. M., and B. T. R. Lewis, Experimental isostasy, 1, Theory of the determination of the earth's isotatic response to a concentrated load, *J. Geophys. Res., 75,* 3357–3365, 1970.

Douglas, B. C., and R. W. Agreen, Sea state bias correction factor from GEOS 3 and SEASAT collinear altimeter data, *Eos Trans. AGU, 62,* 843, 1981.

Hayne, G. S., and D. W. Hancock, Sea-state-related altitude errors in the SEASAT radar altimeter, *J. Geophys. Res., 87,* 3227–3231, 1982.

Heezen, B. C., and D. J. Fornari, Geologic map of the Pacific Ocean, scale, 1:35,000,000, *Initial Rep. Deep Sea Drill. Proj., 30,* 1975.

Lorell, J., E. Colquitt, and R. Anderle, Ionospheric correction for SEASAT altimeter height measurement, *J. Geophys. Res., 87,* 3207–3212, 1982.

McKenzie, D., and C. Bowin, The relationship between bathymetry and gravity in the Atlantic Ocean, *J. Geophys. Res., 81,* 1903–1915, 1976.

McNutt, M., Continental and oceanic isostasy, Ph.D. thesis, Univ. of Calif., San Diego, La Jolla, 1978.

McNutt, M., Compensation of oceanic topography: an application of the response function technique to the Surveyor area, *J. Geophys. Res., 84,* 7589–7597, 1979.

McNutt, M., Influence of plate subduction on isostatic compensation in northern California, *Tectonophysics,* in press, 1982.

McNutt, M., and H. W. Menard, Lithospheric flexure and uplifted atolls, *J. Geophys. Res., 83,* 1206–1212, 1978.

Menard, H. W., and M. McNutt, Evidence for and consequences of thermal rejuvenation, *J. Geophys. Res., 87,* 8570–8580, 1982.

Moritz, H., Fundamental geodetic constants, report, Spec. Stud. Group 5.39, XVII General Assembly, IUGG/IAG, Canberra, 1979.

NOAA, Bathymetric maps of the North Pacific Ocean, scale 4 in. to 1 degree, Natl. Ocean Surv. Seamap Ser., Washington, D.C., 1973.

Saastamoinen, J., Atmospheric correction for the troposphere and stratosphere in radio ranging of satellites, *The Use of Artificial Satellites for Geodesy, Geophys. Monogr. Ser.,* vol. 15, edited by S. W. Henriksen, A. Mancini, and B. H. Chovitz, pp. 247–251, AGU, Washington, D. C., 1972.

Schwank, D. C., and A. R. Lazarewicz, Estimation of seamount compensation using satellite altimetry, *Geophys. Res. Lett., 9,* 907–910, 1982.

Talwani, M., H. R. Poppe, and P. D. Rabinowitz, Gravimetrically determined geoid in the western North Atlantic, Sea surface topography from space, *Tech. Rep. ERL-228-AMOL 7-2,* pt. 2, pp. 1–34, NOAA, Washington, D. C., 1972.

Tapley, B. D., J. B. Lundberg, and G. H. Born, The SEASAT altimeter wet tropospheric range correction, *J. Geophys. Res., 87,* 3213–3220, 1982*a*.

Tapley, B. D., G. H. Born, and M. E. Parke, The SEASAT altimeter data and its accuracy assessment, *J. Geophys. Res., 87,* 3179–3188, 1982*b*.

Walcott, R. I., Flexural rigidity, thickness and viscosity of the lithosphere, *J. Geophys. Res., 75,* 3941–3954, 1970.

Watts, A. B., An analysis of isostasy in the world's oceans, 1, Hawaiian-Emperor seamount chain, *J. Geophys. Res., 83,* 5989–6004, 1978.

Watts, A. B., On geoid heights derived from the GEOS 3 altimeter data along the Hawaiian-Emperor seamount chain, *J. Geophys. Res., 84,* 3817–3826, 1979.

Watts, A. B., J. H. Bodine, and N. M. Ribe, Observations of flexure and the geological evolution of the Pacific Ocean basin, *Nature, 283,* 532–537, 1980.

Wu, S. C., Ionospheric calibration for Seasat altimeter, JPL Internal Document, *Eng. Memo. 315-34,* Jet Propulsion Lab., Pasadena, Calif., 1977.

Wunsch, C., and E. M. Gaposchkin, On using satellite altimetry to determine the general circulation of the oceans with application to geoid improvement, *Rev. Geophys. Space Phys., 18,* 725–745, 1980.

(Received February 18, 1982;
revised August 12, 1982;
accepted September 14, 1982.)